Available online at www.sciencedirect.com
ScienceDirect
International Journal of Pharmaceutics 340 (2007) 207–215
INTERNATIONAL JOURNAL OF PHARMACEUTICS
www.elsevier.com/locate/ijpharm

Pharmaceutical Nanotechnology

UEA I-bearing nanoparticles for brain delivery following intranasal administration

Xiaoling Gao [a,b], Jun Chen [a], Weixing Tao [a], Jianhua Zhu [a], Qizhi Zhang [a], Hongzhuan Chen [b], Xinguo Jiang [a,*]

[a] *Department of Pharmaceutics, School of Pharmacy, Fudan University, Shanghai 200032, PR China*
[b] *Department of Pharmacology, College of Basic Medical Sciences, Shanghai Jiao Tong University, Shanghai 200025, PR China*

Received 10 December 2006; received in revised form 19 March 2007; accepted 22 March 2007
Available online 30 March 2007

Abstract

Surface engineering of nanoparticles with lectins opened a novel pathway to improve the brain uptake of agents loaded by biodegradable PEG-PLA nanoparticles following intranasal administration. Ulex europeus agglutinin I (UEA I), specifically binding to L-fucose, which is largely located in the olfactory epithelium, was selected as a promising targeting ligand and conjugated onto the PEG-PLA nanoparticles surface with an optimized protocol relying on maleimide-mediated covalent binding technique. The *in vivo* results in rats suggested that UEA I modification at the nanoparticles surface facilitated the absorption of a fluorescent marker—6-coumarin associated with the nanoparticles into the brain following intranasal administration with significant increase in the area under the concentration–time curve (about 1.7 times) in different brain tissues compared with that of coumarin incorporated in the unmodified ones. UEA I-conjugation also elevated the brain-targeting efficiency of nanoparticles. Inhibition experiment of specific sugar suggested that the interactions between the nasal mucosa and the lectinised nanoparticles were due to the immobilization of carbohydrate-binding pockets on the surface of the nanoparticles. Distribution profiles of UEA I-modified nanoparticles indicated their higher affinity to the olfactory mucosa than to the respiratory one. Therefore, the UEA I-modified nanoparticles might serve as potential carriers for brain drug delivery, especially for mental therapeutics with multiple biological effects.

Keywords: Brain targeting; Nanoparticles; Ulex europeus agglutinin I; Intranasal administration

1. Introduction

Drug delivery to the brain is made difficult by the presence of the blood-brain barrier (BBB), which is formed by tight junctions within the capillary endothelium of the vertebrate brain (Pardridge, 1991). A great deal of efforts, therefore, have been made in developing ways to open, defeat or circumvent the BBB in order to deliver drugs from blood to brain. Intranasal administration offers a non-invasive alternative route to the central nervous system (CNS) for drug delivery, effectively bypassing the BBB (Graff and Pollack, 2005). Indeed, the past few years have witnessed a sharp increase in the amount of research on the nasal pathway for the CNS drug delivery (Graff and Pollack, 2005). However, the total amount of drugs accessing the brain were reported to be low, especially for nasally applied biotech drugs such as peptides, proteins and DNA, which were poorly absorbed and highly susceptible to the harmful environment of the nasal cavity (Chen et al., 1998; Kim et al., 2000; Dufes et al., 2003). The incorporation of these drugs into nanoparticles might be a promising approach, since colloidal formulations have been shown to protect them from the degrading milieu in the nasal cavity and facilitate their transport across the mucosal barriers (Vila et al., 2002). Besides, the resident time of nanoparticles in nasal cavity is limited because of mucociliary clearance (e.g. particle clearance within the nose every 15–20 min), which is not available for the complete absorption of the formulation (Vyas et al., 2005). This made bioadhesive formulations with enhanced permeability a better alternative.

The bioadhesive delivery system can be obtained by means of surface modification of drug carriers with biological ligands, which recognize and adhere to specific chemical structures on the surface of cells, thus facilitating absorption of the delivery

* Corresponding author. Tel.: +86 21 54237381; fax: +86 21 54237381.
E-mail address: xgjiang@shmu.edu.cn (X. Jiang).

0378-5173/$ – see front matter © 2007 Published by Elsevier B.V.
doi:10.1016/j.ijpharm.2007.03.039

system. A good example of this is that lectins, proteins or glycoproteins of nonimmunological origin, which specifically recognize sugar molecules and bind the glycosylated membrane components, were widely used to conjugate with colloidal carrier systems, such as liposomes or nanoparticles to improve oral drug absorption (Bies et al., 2004). Our recent work suggested that wheat germ agglutinin (WGA) modification on the surface of poly(ethylene glycol)-poly(lactic acid) (PEG-PLA) nanoparticles facilitated the uptake of fluorescence tracer embedded in the nanoparticles in the CNS following intranasal administration (Gao et al., 2006). Ulex europeus agglutinin I (UEA I), specifically binding to L-fucose, which is largely located in the olfactory epithelium (Lundh et al., 1989), was widely used as a neuronal marker (Gheri et al., 1991; Pellier and Astic, 1994). Previous research also suggested that UEA I-bearing liposomes exhibited effective targeting to Peyer's patch (Chen et al., 1996). Thus, the aim of this contribution was to present a protocol for surface engineering of PEG-PLA nanoparticles with UEA I and to evaluate its ability to mediate drug delivery to the brain following intranasal administration. To achieve this goal, maleimide-PEG-PLA was blended with PEG-PLA to prepare nanoparticles by simple emulsion/solvent evaporation. The resulting nanoparticles were then functionalized with thiolated WGA by taking advantage of the thiol group coupling activity of maleimide. In the study of the blood and brain uptake of the functionized nanoparticles, a lipophilic fluorescent probe with high sensitivity, 6-coumarin, which was widely used in the *in vitro* and *in vivo* experiments (Desai et al., 1997; Panyam and Labhasetwar, 2003; Lu et al., 2005), was incorporated into the nanoparticles, and the blood and brain tissue concentrations of the fluorescent marker associated to UEA I-conjugated nanoparticles were detected with a high performance liquid chromatography (HPLC)-fluorescence detection method.

2. Materials and methods

2.1. Materials and animals

The copolymers of methoxy-PEG-PLA (MePEG-PLA) and maleimide-PEG-PLA were synthesized by the ring opening polymerization of D,L-lactide (99.5% pure, PURAC) initiated by MePEG (M_W 3000 Da, SUNBRIGHT^{TM} MEH-30H, NOF Corporation, Lot no. 14530, Japan) and maleimide-PEG (M_W 3400 Da, NEKTAR^{TM}, Lot no. PT-08D-16, Huntsville, AL, USA), respectively, using stannous octoate as catalyst (Y. Zhang et al., 2004; Gao et al., 2006). UEA I and L-fucose were obtained from Sigma (USA), 6-coumarin from Aldrich (USA), 2-iminothiolane hydrochloride (2-IT) from Sigma (USA) and 5, 5-dithiobis (2-nitrobenzoic acid) (Ellman's reagent) from Acros (Belgium). Rabbit anti-nerve-specific enolase polyclonal antibody and Cy3-conjugated goat-anti-rabbit IgG were purchased from Wuhan Boster Biological Technology Ltd. Double-distilled water was prepared using a Millipore Simplicity System (Millipore, Bedford, USA). All the other materials were of analytical reagent grades and used without further purification.

Sprague–Dawley rats (180–220 g) were obtained from the Experimental Animal Center of Fudan University and maintained at 22 ± 2 °C on a 12 h light–dark cycle with access to food and water *ad libitum*. And animal experiments were carried out in compliance with the protocol of Animal Use and Care by the Medical Center of Fudan University.

2.2. Preparation of UEA I-conjugated PEG-PLA nanoparticles (UEA-NP)

2.2.1. Preparation of 6-coumarin-loaded PEG-PLA nanoparticles

PEG-PLA nanoparticles (NP) were prepared with a blend of maleimide-PEG-PLA and MePEG-PLA using the emulsion/solvent evaporation technique described by Tobio et al. (1998). Briefly, 50 μl of water was emulsified by sonication (220 W, 30 s) on ice using a probe sonicator (Scientz Biotechnology Co. Ltd., China) in 1 ml of a solution of 25 mg/ml of blend of maleimide-PEG-PLA and MePEG-PLA at different ratios in dichloromethane containing 2 mg/ml of 6-coumarin. This primary emulsion was then emulsified by sonication (220 W, 30 s) on ice in a 2 ml of 1% aqueous sodium cholate solution. And the w/o/w emulsion obtained was further diluted into 25 ml of a 0.5% aqueous sodium cholate solution under moderate magnetic stirring. Five minutes later, dichloromethane was evaporated at low pressure at 30 °C using Büchi rotavapor R-200 (Büchi, Germany). Then the nanoparticles were centrifuged at 21,000 × *g* for 45 min using TJ-25 centrifuge (Beckman Counter, USA) equipped with A-14 rotor. The supernatant discarded, and the obtained nanoparticles were subjected to a 1.5 cm × 20 cm sepharose CL-4B column and eluted with 0.05 M HEPES buffer (pH 7.0) containing 0.15 M NaCl to remove the 6-coumarin unentrapped or adsorbed to the exterior of the nanoparticles.

2.2.2. Surface modification of the nanoparticles

UEA I was radio labeled with iodogen methods as described previously (Sobal et al., 2004), purified, mixed with unlabeled lectin and thiolated for 60 min with a predetermined molar excess of 2-iminothiolane in 0.15 M sodium borate buffer, pH 8 supplemented with 0.1 mM EDTA. The product was then purified with Hitrap^{TM} Desalting column (Amersham Pharmacia Biotech AB, Sweden) with the protein fractions collected and introduced thiol groups determined spectrophotometrically (λ = 412 nm) with Ellman's reagent (Ellman, 1959).

Then the thiolated protein, contained a trace amount of ^{125}I-labeled UEA I, was incubated with different amounts of nanoparticles to react at room temperature for 4–16 h. The unconjugated UEA I was separated from nanoparticles by Sepharose CL-4B column chromatography.

2.3. Morphology and particle size

The morphological examination of nanoparticles was performed by transmission electron microscopy (TEM) (H-600, Hitachi, Japan) following negative staining with sodium phosphotungstate solution. The mean diameter of the nanoparticles was determined by dynamic light scattering (DLS) analysis

using Zeta Potential/Particle Sizer NICOMP™ 380 ZLS (Santa Barbara, California, USA) with He–Ne lamp at 632.8 nm.

2.4. Determination of the number of lectin on the surface of nanoparticles and the conjugation efficiency

In order to determine the lectin density on the surface of the resulting particles, UEA I was radio labeled and the amount of UEA I at the particle surface was determined by γ-counting (SN-682 Gamma ratioimmunoassay counter, Ri Huan Instrument Factory of Shanghai, Shanghai, China). The UEA-NP concentration was determined by turbidimetry using UV2401 spectrophotometer at 350 nm (Shimadzu, Japan). The average number of lectin molecules conjugated per particle was calculated by dividing the number of lectin with the calculated average number (n) of nanoparticles using the methods described by Olivier et al. (2002):

$$n = \frac{6m}{\pi} \times D^3 \times \rho \quad (1)$$

where m is the nanoparticle weight, D the number-based mean nanoparticle diameter determined by DLS, ρ the nanoparticle weight per volume unit (density), estimated to be 1.1 g/cm^3 (Olivier et al., 2002).

The conjugation efficiency (CE%) was also calculated to determine the percentage of lectin conjugated on the nanoparticle surface:

$$\text{CE\%} = \frac{\text{amount of lectin conjugated at the nanoparticle surface}}{\text{total amount of lectin added}} \times 100\% \quad (2)$$

2.5. Determination of the encapsulation efficiency and loading capacity

To measure the 6-coumarin content, a predetermined amount of nanoparticles was analyzed using the extraction protocol and HPLC analysis method described in Section 2.7.2. The measurements were performed in triplicate, and the encapsulation efficiency and 6-coumarin loading in nanoparticles were calculated as indicated below:

$$\text{encapsulation efficiency (\%)} = \frac{\text{amount of 6-coumarin in nanoparticles}}{\text{total amount of 6-coumarin added initially}} \times 100\% \quad (3)$$

$$\text{loading (\%)} = \frac{\text{amount of 6-coumarin in nanoparticles}}{\text{nanoparticles weight}} \times 100\% \quad (4)$$

2.6. In vitro release study of 6-coumarin from UEA-NP

In vitro release experiments of 6-coumarin from the nanoparticles were performed under different pH conditions at 37 °C in order to evaluate if the fluorescence tracer remained associated with the particles during a 24-h incubation period. Buffers of pH 4 and 7.4 were selected for the *in vitro* release investigations to represent the pH presented in the endo-lysosomal compartment and physiologic pH, respectively. 6-coumarin-loaded UEA-NP were dispersed in pH 4 and 7.4 PBS at a nanoparticles concentration of 0.625 μg/ml with a 6-coumarin concentration of about 25 ng/ml to provide sink condition, divided averagely into sixty samples (0.5 ml/sample), respectively, and incubated at 37 °C immediately. Periodic samples (0 min, 5 min, 15 min, 30 min, 1 h, 2 h, 4 h, 8 h, 12 h, 24 h, $n = 3$) were subjected to centrifugation at 21,000 × g for 45 min and the supernatant was further diluted with one-fold volume of methanol and analyzed for the released amount of 6-coumarin. Furthermore, in order to reduce the influence of time-related quenching of the fluorescence, three additional periodic samples were simultaneously taken for the determination of the total amount of fluorescence retained in the samples at each time point using the extraction protocol and HPLC analysis method described in Section 2.7.2. The cumulative release percentage (CR%) of 6-coumarin from nanoparticles at each time point was calculated using the following equation:

$$\text{CR\%} = \frac{\text{amount of 6-coumarin in the supernatant}}{\text{total amount of 6-coumarin}} \times 100\% \quad (5)$$

2.7. Nasal absorption, brain uptake and brain-targeting efficiency of UEA-NP

2.7.1. Animal experiments

Thirty-two rats were given an intranasal administration of 6-coumarin-loaded UEA-NP. While in administration, the conscious rats were fixed in a prostrate position, and the UEA-NP were administered at the openings of the nostrils using a polyethylene 10 (PE 10) tube attached to a microlitre syringe. The procedure was performed gently and slowly, which lasted for about 2 min, allowing the rats to inhale all of the preparations. Each animal received a total of about 0.5 mg (2.5 mg/kg) of nanoparticles in 20 μl (10 μl each nostril) of 0.01 M HEPES buffer (pH 8.5) containing 0.1 mM $CaCl_2$, which was used to provide an optimal condition for the binding between lectin and sugar) (Teichberg et al., 1988).

At each of the time points (0.25, 0.5, 1, 2, 4, 8, 12 and 24 h) following administration, four animals were euthanized and decapitated, with their skulls cut open and brain tissue samples excised in the order of the cerebrum, cerebellum, olfactory tract and olfactory bulb. Blood was collected with a syringe and a coarse needle from the trunk and put into the tubes with heparin.

2.7.2. Analytical procedures

The samples for analysis were prepared as described previously (Gao et al., 2006). In brief, the brain samples were homogenized with three-fold volumes of distilled water. Then 10 μl of 7-coumarin (70 ng/ml, internal standard) and 1 ml of n-hexane were added to 200 μl of the homogenate to extract the fluorescent dye from the samples. Intensely vortexed for

5 min, the mixture was subjected to centrifuge at 15,000 × *g* for 10 min. The supernatant was collected and evaporated under a stream of nitrogen at 40 °C. The residue was dissolved in 50 μl of methanol with 20 μl injected into the HPLC system. The whole blood samples were homogenized without the addition of water and treated with the same method.

The fluorescent tracer concentrations in different brain tissues and the blood were analyzed by an HPLC system (Shimadzu Scientific Instrument Inc., Japan) consisted of a pump (Model LC-10AT) and a fluorescence detector (Model RF-10AXL; $\lambda_{ex} = 465$ nm, $\lambda_{em} = 502$ nm). With a reversed-phase column, Dikma Diamonsil® C_{18} (250 mm × 4.6 mm, 5 μm), the separations were achieved using methanol and water at the ratio of 96:4 as the mobile phase with a flow rate of 1.5 ml/min and column temperature of 35 °C.

2.7.3. Data analysis

The results were plotted as 6-coumarin concentration–time curves in the blood and brain tissues. The C_{max} and t_{max} values following intranasal administration were read directly from the concentration–time profiles. The area under the curve (AUC) was calculated by the trapezoidal method without extrapolation to infinity. The variance for the $AUC_{0\rightarrow t}$ was estimated using the method of Yuan (1993). Clearance rate (Cl) of 6-coumarin carried by UEA-NP from the blood and brain tissues following intranasal administration was calculated using 3p87 Pharmacokinetic Program (Beijing, China). The data obtained was compared with that after intranasal application of 6-coumarin-loaded unmodified nanoparticles (NP), which had been presented in our previous work (Gao et al., 2006).

Brain-targeting efficiency of UEA-NP was evaluated with the method mentioned previously (Q. Zhang et al., 2004), where drug targeting efficiency (DTE), represented the time-average partitioning ratio of the target tissues to the blood, was calculated as follows:

$$\mathrm{DTE} = \frac{\mathrm{AUC}_{\mathrm{brain},0-24\,\mathrm{h}}}{\mathrm{AUC}_{\mathrm{blood},0-24\,\mathrm{h}}} \quad (6)$$

and compared with that of wheat germ agglutinin-conjugated nanoparticles (WGA-NP) and NP (Gao et al., 2006).

For multiple-group comparison, one-way ANOVA was used following Student–Newman–Keuls post hoc test. For two-group comparison, a two-sided unpaired Student's *t*-test was employed. Differences were considered statistically significant at $P < 0.05$.

2.8. Specificity of uptake of UEA-NP in the nasal cavity

The specific nature of the uptake of the lectin-modified nanoparticles was determined by inhibition experiment of specific sugar. UEA-NP (25 mg/ml) was preincubated with excess L-fucose (100 mM) at 4 °C overnight in 0.01 M HEPES buffer (pH 8.5) containing 0.1 mM $CaCl_2$, then the mixture was given to four animals (20 μl per rat, 10 μl per nostril). Four hours later, the animals were euthanized with brain tissues and blood samples collected and analyzed with the methods mentioned above. Animals treated with the same amount of UEA-NP ($n = 4$) and NP ($n = 4$) were used as controls, respectively. The statistical differences between groups were assessed using one-way ANOVA followed by Student-Newman-Keuls post hoc test.

2.9. Distribution of UEA-NP in the nasal mucosa

In order to investigate the distribution profile of UEA-NP in the nasal mucosa, 0.075% (g/g) of 6-coumarin was entrapped into nanoparticles as a fluorescence probe using the method described above. Having received a total of about 0.5 mg (2.5 mg/kg) of nanoparticles in 50 μl 0.01 M HEPES buffer (pH 8.5) containing 0.1 mM $CaCl_2$, each animal was fixed by heart perfusion 2 h after administration. The nasal cavity was isolated and immersed in 4% paraformaldehyde for 24 h. Following decalcification, the nasal cavity was cut into five slices approximately 2–3 mm thick (Jansson et al., 2005), which were then dehydrated in sucrose solution, embedded in Tissue-Tek® O.C.T compound (Sakura Finetek, USA) and stored at −70 °C until sectioned frozen. Then the sections were transferred to microscope slides and the olfactory mucosa was labeled by using anti-nerve-specific enolase as the primary antibody (Inamitsu et al., 1990) according to the procedure described by Ohtake et al. (2003). Briefly, the sections were incubated for 20 min with normal goat serum, and then for 30 min at 37 °C and overnight at 4 °C with 1:200 rabbit anti-nerve-specific enolase monoclonal antibody. Rinsed in 0.01 M PBS (pH 7.4) three times for 5 min, the sections were incubated with 1:400 Cy3-conjugated goat-anti-rabbit IgG before counterstained with DAPI following three times of rinsing in 0.01 M PBS. Finally, they were observed under a fluorescence microscope (Olympus IX71) with three optical filters (6-coumarin: XF100-2; DAPI: XF113-2; Cy3: XF108-2), respectively. The images were taken and colored with Image-Pro Plus.

3. Results

3.1. Influence of different parameters on the characteristics of UEA-NP during nanoparticle preparation and surface modification

3.1.1. Influence of the amount of maleimide-PEG-PLA

To investigate the influence of the number of active groups on the lectin density at the nanoparticle surface, constant total amount of polymers were used to prepare the nanoparticles with increased fraction of maileimide-PEG-PLA. The results suggested that the number of lectin at the surface of the nanoparticles increased concurrently with the increasing ratio of maleimide-PEG-PLA to MePEG-PLA. However, the optimized ratio should be set at around 1:9 since a lower ratio might result in the decrease of ligand density, which might lead to loss of biorecognitive interactions, while a higher one (e.g. 1:5) might provoke crosslink or agglomeration of the particles, resulting in enlarged particle size (Table 1).

3.1.2. Influence of the amount of 2-iminothiolane

Considering the flexibility of targeting ligand might affect its receptor-binding capacity (Olivier et al., 2003), one thiol

Table 1
Influence of the ratio of maleimide-PEG-PLA to MePEG-PLA on the particle size and lectin density on the surface of UEA-NP

The ratio of maleimide-PEG-PLA to MePEG-PLA	Particle size (nm)	Lectin per nanoparticle
1:9	111.0 ± 9.8	138 ± 12
1:5	195.6 ± 17.5	1196 ± 57

UEA-NP, UEA I-conjugated nanoparticles. The lectins were thiolated for 60 min with a 60:1 molar excess of 2-iminothiolane, purified, and then incubated with the activated nanoparticles at a molar ratio of thiolated lectin: maleimide at 1:3 to react for 10 h.

Table 2
Influence of the amount of 2-iminothiolane on the number of thiol group on each lectin

The ratio of 2-iminothiolane to lectin	Number of thiol group per lectin
40:1	0.73
60:1	1.02
80:1	1.43

group per lectin was optimal. Therefore, the molar ratio of UEA: 2-iminothiolane at 1:60 was optimized (Table 2).

3.1.3. Influence of the amount of thiolated lectin

To find out whether the lectin density can be adjusted by the amount of lectin added, the activated nanoparticles were incubated with increasing amounts of thiolated lectin and the conjugation number, the conjugation efficiency as well as the size of the particles were determined.

The amount of lectin bound to the surface increased concurrently with the increasing amount of thiolated lectin (Table 3). However, the addition of too much lectin (e.g. the ratio of thiolated lectin to maleimide-PEG-PLA at 1:1) resulted in the reduction of conjugation efficiency from 71.20% to 47.53% and the increase of average particle size from 111.5 to 152 nm. Hence, the ratio at 1:3 was optimized.

3.1.4. Influence of the incubation time

To check whether the extended incubation with the lectin exerts some influence on the particle size, conjugation efficiency and lectin density at the particle surface, the thiolated lectin was allowed to interact with nanoparticles for different incubation time.

Significant increase in ligand density and conjugation efficiency concurrent with constant particle size was observed with the extension of the coupling time from 4 to 10 h. And higher lectin density as well as larger particle size, mainly due to agglomeration of the particles or crosslink of the thiolated protein, were produced by further prolonged incubation (more than 12 h) (Table 4). Therefore, the coupling of the biorecognitive ligand onto the nanoparticles surface should be performed for 8–10 h.

3.2. In vitro release of 6-coumarin from UEA-NP and NP

Approximately 4% (w/w) 6-coumarin loading and 50% encapsulation efficiency were found in the nanoparticles. The results of the *in vitro* release study conducted in pH 4 and 7.4 PBS at 37 °C, consistent with previous studies (Desai et al., 1997) showed that only 3.86% and 3.03% of 6-coumarin was released from UEA-NP, respectively, after a 24-h incubation period. These data clearly suggested that almost all the fluorescent tracer retained associated with the nanoparticles in the experimental period.

Table 3
Influence of the amount of thiolated lectin added on the particle size, conjugation efficiency and lectin density at the surface of UEA-NP

The ratio of thiolated lectin to maleimide-PEG–PLA	Particle size (nm)	Conjugation efficiency (%)	Lectin per nanoparticle
1:1	152 ± 18.8	47.53 ± 2.76	998 ± 42
1:3	111.0 ± 9.8	50.68 ± 3.40	138 ± 12
1:5	111.5 ± 11.9	71.20 ± 3.04	117 ± 6

UEA-NP, UEA I-conjugated nanoparticles. The lectins were thiolated in reaction for 60 min with a 60:1 molar excess of 2-iminothiolane, purified, and then incubated with the activated nanoparticles (the ratio of maleimide-PEG-PLA: Me PEG-PLA 1:9) to react for 10 h.

Table 4
Influence of the incubation time on the particle size, conjugation efficiency and lectin density at the surface of UEA-NP

Incubation time (h)	Particle size (nm)	Conjugation efficiency (%)	Lectin per nanoparticle
4	88.6 ± 6.2	25.57 ± 1.57	35 ± 7
8	103.2 ± 6.5	58.12 ± 2.88	127 ± 11
10	111.0 ± 9.8	50.68 ± 3.40	138 ± 12
12	121.8 ± 4.8	46.10 ± 3.25	166 ± 12
16	168.5 ± 8.7	47.32 ± 4.93	439 ± 11

UEA-NP, UEA I-conjugated nanoparticles. The lectins were thiolated in reaction for 60 min with a 60:1 molar excess of 2-iminothiolane, purified, and then incubated with the activated nanoparticles (the ratio of maleimide-PEG-PLA: Me PEG-PLA 1:9) at a molar ratio of thiolated lectin: maleimide at 1:3 for 4–16 h.

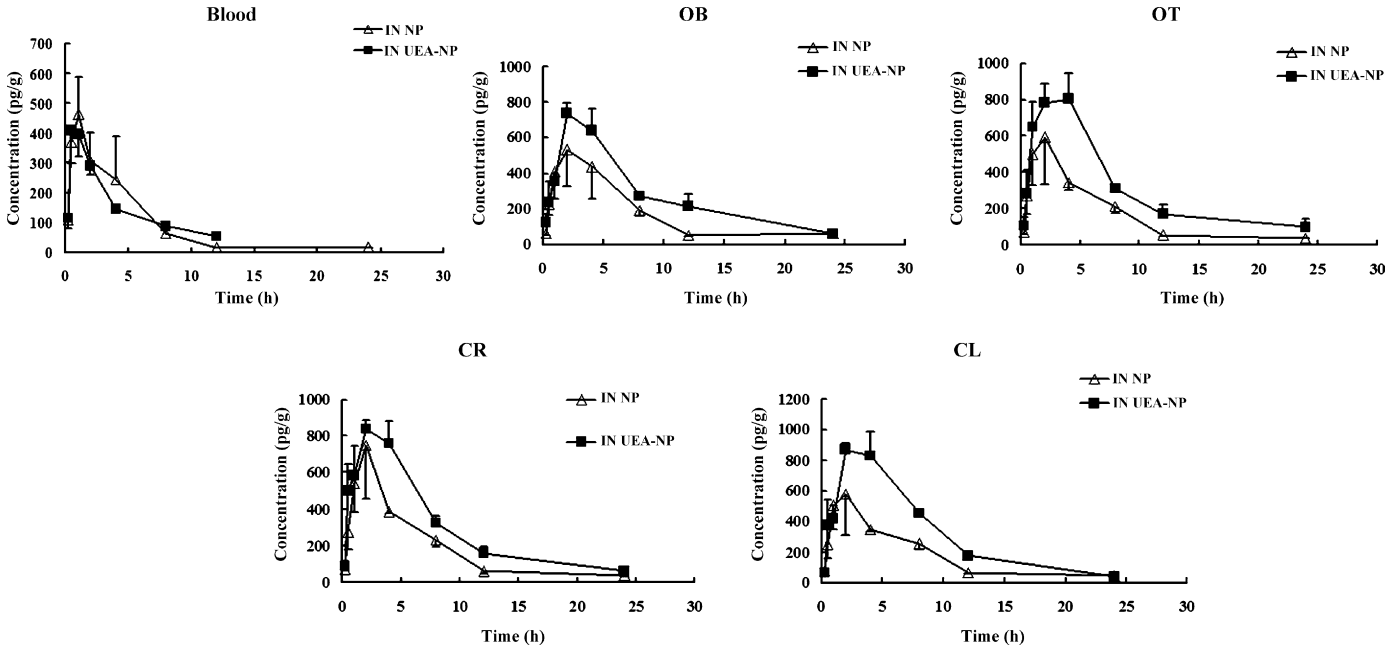

Fig. 1. Blood and brain tissue concentration–time profiles of 6-coumarin following intranasal administration of coumarin-loaded UEA-NP and NP at the dose of 2.5 mg/kg of nanoparticles. Data represented the mean ± S.E.M. UEA-NP, UEA I-conjugated nanoparticles; NP, unmodified nanoparticles; OB, olfactory bulb; OT, olfactory tract; CR, cerebrum; CL, cerebellum.

3.3. Nasal absorption, brain uptake and brain-targeting efficiency following intranasal administration

To evaluate the absorption of the functionized nanoparticles into the blood and brain, 6-coumarin was incorporated into the nanoparticles, and the concentrations of the fluorescent marker in the blood and brain samples were detected with a validated HPLC-fluorescence detection method.

The data suggested that although the systemic absorption of coumarin associated with UEA-NP displayed a faster absorption phase with the highest concentration observed 30 min after the administration (Fig. 1, Table 5), the $AUC_{0–24\,h}$ of coumarin carried by UEA-NP was about 20% less than that entrapped in NP ($P < 0.05$) (Table 5). On the contrary, UEA modification facilitated the uptake of fluorescence tracer embedded in the nanoparticles in the CNS with 30% increase in C_{max} at the time point of 2 h (Fig. 1, Table 5) and 70% increase in $AUC_{0–24\,h}$ ($P < 0.05$) (Table 5). Furthermore, the clearance rate of 6-coumarin carried by UEA-NP from different brain tissues was lower than that following intranasal administration of 6-coumarin-loaded NP.

In order to evaluate the brain-targeting efficiency of UEA-NP, DTE was calculated with the method described previously, and compared with that of WGA-NP and NP. The highest DTE value was obtained following intranasal administration of UEA-NP, WGA-NP the second and NP the lowest ($P < 0.05$) (Table 6), indicating that both lectins functionization facilitated brain targeting of the nanoparticles and UEA-modified nanoaprticles might serve as the most promising carriers with elevated brain-targeting ability.

Table 5
Pharmacokinetic parameters of 6-coumarin following an intranasal administration of coumarin-loaded UEA-NP and NP at the dose of 2.5 mg/kg of nanoparticles

Formulation	Tissue	C_{max} (pg/ml or pg/g)	T_{max} (h)	$AUC_{0\text{-}24h}$ (pg h/ml or pg h/g)	Cl (L/h)
UEA-NP	Blood	407.55 ± 109.30[a,c]	0.5	1733.66 ± 103.89[b,*]	0.13
	OB	738.72 ± 59.20[*]	2	6566.89 ± 641.07[*]	0.07
	OT	782.58 ± 106.86[*]	2	7041.10 ± 660.04[*]	0.03
	CR	841.95 ± 47.62	2	7141.02 ± 500.38[*]	0.08
	CL	872.39 ± 36.28[*]	2	7375.06 ± 534.51[*]	0.07
NP	Blood	464.75 ± 124.71	1	2179.41 ± 478.46	0.28
	OB	535.17 ± 205.80	2	3739.89 ± 671.86	0.15
	OT	596.01 ± 261.42	2	4025.55 ± 458.31	0.18
	CR	753.53 ± 296.65	2	4503.18 ± 492.54	0.19
	CL	578.30 ± 269.66	2	4305.05 ± 464.25	0.22

UEA-NP, UEA I-conjugated nanoparticles; NP, unmodified nanoparticles; OB, olfactory bulb; OT, olfactory tract; CR, cerebrum; CL, cerebellum; Cl, clearance rate.
[a] Mean ± S.E.M.
[b] Mean ± S.D.
[*] Significantly different from NP, $P < 0.05$.

Table 6
Drug targeting efficiency of coumarin-loaded WGA-NP, UEA-NP and NP at the dose of 2.5 mg/kg of nanoparticles following intranasal administration in rats

	WGA-NP	UEA-NP	NP
DTE			
OB	2.33 ± 0.48[a,b]	3.79 ± 0.43[b,c]	1.72 ± 0.49
OT	2.67 ± 0.55[b]	4.06 ± 0.45[b,c]	1.85 ± 0.46
CR	2.93 ± 0.60[b]	4.12 ± 0.39[b,c]	2.07 ± 0.51
CL	2.77 ± 0.62[b]	4.25 ± 0.40[b,c]	1.98 ± 0.48

WGA-NP, WGA-conjugated nanoparticles; UEA-NP, UEA I-conjugated nanoparticles; NP, unmodified nanoparticles; DTE, Drug targeting efficiency; OB, olfactory bulb; OT, olfactory tract; CR, cerebrum; CL, cerebellum.
[a] Mean ± S.D.
[b] Significantly different from NP, $P < 0.05$.
[c] Significantly different from WGA-NP, $P < 0.05$.

3.4. Specificity of uptake of UEA-NP by nasal mucosa

The specificity of nasal absorption of UEA-NP was tested by inhibition experiment of specific sugar. Four hours following the administration, the brain concentrations of coumarin carried by UEA-NP preincubated with excess specific sugars, were slightly higher than that of fluorescent dye entrapped in NP but lower than that of 6-coumarin associated with UEA-NP ($P < 0.1$) (Table 7), suggesting that the specific interactions between the nasal mucosa and the lectinised nanoparticles might be resulted from the immobilization of carbohydrate-binding pockets on the surface of the nanoparticles.

3.5. Distribution of UEA-NP in the nasal mucosa

In order to investigate the distribution of UEA-NP in the nasal mucosa, the olfactory mucosa was labeled with anti-nerve-specific enolase antibody (Fig. 2A and C red, right). Two hours after intranasal administration of 6-coumarin-loaded UEA-NP, most green fluorescence was observed on the surface of olfactory mucosa and in the connective tissues surrounding the olfactory nerve bundles (Fig. 2B and C right). On the contrary, in the same visual field, significantly less green fluorescence was detected on the respiratory mucosa (Fig. 2B and C left). But in the case of intranasal administration of NP, comparative amounts of green fluorescence were observed on the olfactory (Fig. 2D) and respiratory mucosa (Fig. 2E). These telling results suggested that the affinity of UEA-NP to the olfactory mucosa was greater than that to the respiratory one, but in the case of NP, similar affinity to the olfactory and respiratory area was observed.

4. Discussion

UEA-NP was prepared using the protocol described previously (Gao et al., 2006). In this contribution, the protocol was optimized based on the following endpoints: lectin density at the particle surface, particle size and conjugation efficiency, which were chosen for the following reasons: previous researches suggested that the ligand density played an important role in facilitating cell uptake of the modified nanoparticles (Russell-Jones et al., 1999; Gref et al., 2003); cell uptake of particles were also related to the particle size (Desai et al., 1997; Vila et al., 2005); conjugation efficiency was determined to evaluate the availability of the lectin added. The data suggested that the optimized ratio of maleimide-PEG-PLA to MePEG-PLA was around 1:9, the molar ratio of lectin: 2-iminothiolane 1:60, the thiolated lectin to maleimide ratio 1:3 and the conjugation time lasted for 8–10 h.

As indicated by the *in vivo* data, in the case of systemic absorption, the $AUC_{0-24\,h}$ of coumarin carried by UEA-NP was about 20% less than that of NP. But in the case of uptake in the brain tissues, UEA I modification at the nanoparticles surface facilitated the uptake of fluorescence tracer embedded in the nanoparticles in the CNS with 70% increase in $AUC_{0-24\,h}$. Furthermore, the clearance of 6-coumarin carried by UEA-NP from the CNS was slower than that following intranasal administration of NP. These results might be brought from the fact that the conjugated lectin induced strong mucoadhesion of a prolonged duration, or a close contact of the nanoparticles with the mucosal cells so as to produce a stronger penetration. Lectin might also trigger or facilitate the active transport of nanoparticles through the nasal mucosa (Bies et al., 2004). The involvement of the specific carbohydrate-binding motif on the surface of the lectin-grafted nanoparticles was demonstrated by the competitive assay with excess specific sugars in the contribution.

These results were consistent with our previous data about WGA-NP for brain delivery following intranasal administration (Gao et al., 2006). However, different enhancing patterns

Table 7
Blood and brain concentration of 6-coumarin 4 h after an intranasal administration of coumarin-loaded UEA-NP, UEA-NP preincubated with exess L-fucose and NP at the dose of 2.5 mg/kg of nanoparticles

$Concentration_{4\,h}$ (pg/ml or pg/g)			
	UEA-NP ($n = 4$)	UEA-NP preincubated with excess specific sugars ($n = 4$)	NP ($n = 4$)
Blood	145.30 ± 5.66[a]	127.06 ± 29.44	242.56 ± 104.63
OB	641.05 ± 88.94	564.76 ± 67.84	438.56 ± 184.30
OT	803.57 ± 108.21[*]	470.80 ± 28.26[*]	344.81 ± 42.59[*]
CR	761.62 ± 91.40	567.61 ± 56.31	388.43 ± 13.40
CL	828.65 ± 120.40[*]	445.05 ± 54.01[*]	352.34 ± 17.64[*]

UEA-NP, UEA I-conjugated nanoparticles; NP, unmodified nanoparticles; OB, olfactory bulb; OT, olfactory tract; CR, cerebrum; CL, cerebellum.
[a] Mean ± S.E.M.
[*] The data were statistically different based on ANOVA test followed by Student–Newman–Keuls post hoc test ($P < 0.1$).

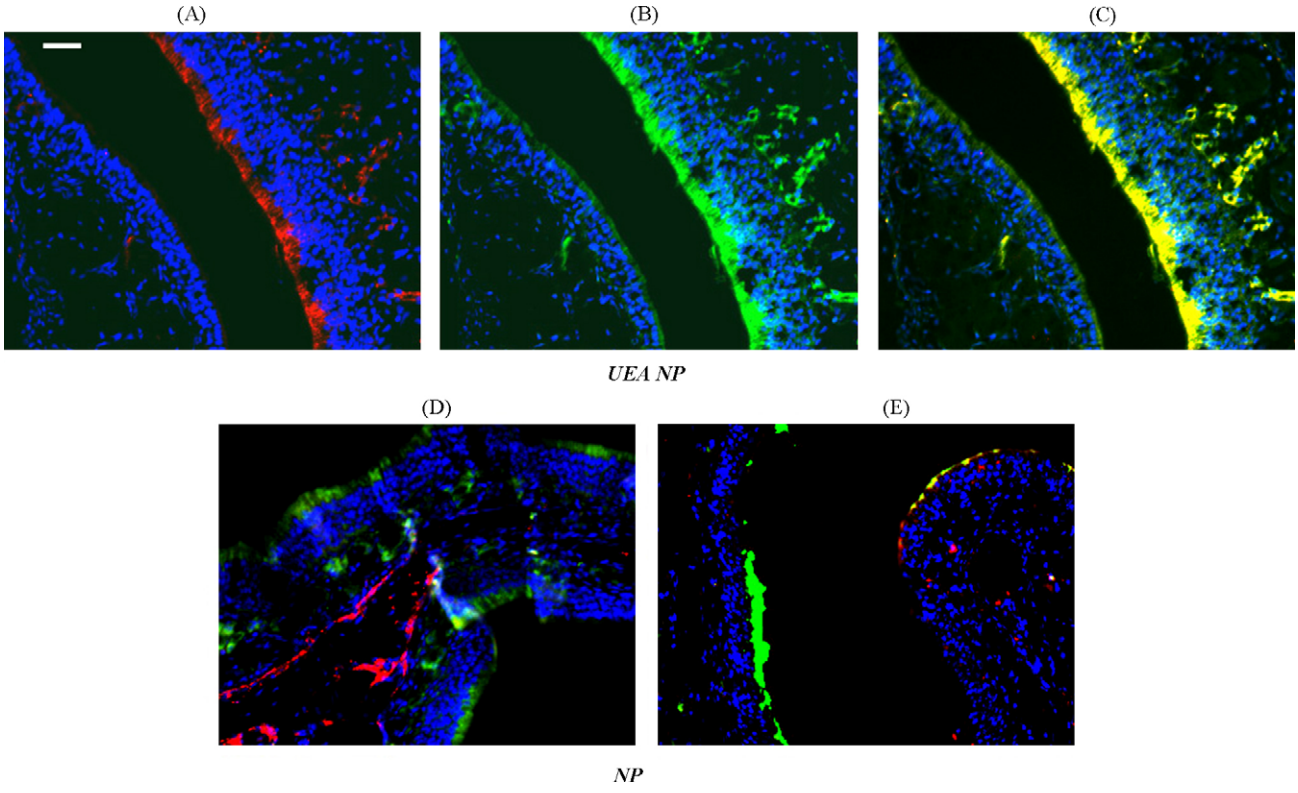

Fig. 2. Distribution of 6-coumarin-loaded UEA-NP and NP in the nasal mucosa 2 h following intranasal administration. (A) Olfactory mucosa stained with anti-nerve-specific enolase antibody (right). Olfactory receptor cells and olfactory nerve bundles positive stained; (B) high level of green fluorescence located in the olfactory mucosa (right). In the same visual field, significantly less green fluorescence detected on the respiratory mucosa (left); (C) overlap of (A) and (B); (D and E) comparative amounts of green fluorescence observed on the olfactory (D) and respiratory (E) mucosa following intranasal administration of NP. Scale bar, 50 μm. (For interpretation of the references to color in this figure legend, the reader is referred to the web version of the article.)

were observed between the two lectinised nanoparticles: WGA modification facilitated the absorption of the fluorescent tracer into both the brain and the circulation, while UEA I-conjugation only improved the absorption of that into the brain and presented better brain-targeting efficiency with markedly elevated DTE, suggesting that UEA-modified nanoaprticles might serve as promising carriers with better brain-targeting efficiency, especially for mental therapeutics characterized by multiple biological effects. Since the preparation protocol for both of the lectin-conjugated nanoparticles was optimized, the size of the particles and ligand density at the nanoparticle surface were controlled within the same range, the difference could be largely attributed to the kinds of lectin selected and their specific substrates with different distribution patterns in the nasal mucosa. It was believed that the nasal mucosa was composed of respiratory region, which had the highest degree of vascular and was mainly responsible for drug absorption into the circulation, and olfactory mucosa, which played a vital role in the transport of drugs into the brain and CSF (Illum, 2000) and the two regions presented different lectin-binding profiles. WGA, specifically binding to *N*-acetyl-D-glucosamine and sialic acid, showed a great binding affinity to the olfactory epithelium but a moderate one to the respiratory epithelium (Takami et al., 1994; Melgarejo Moreno et al., 1998) while UEA I, specifically binding to L-fucose, was widely used as a neuronal marker, intensely labeled the entire nerve cell population in the vomeronasal organ and the olfactory epithelium (Lundh et al., 1989). Hence, it was easy to understand why WGA modification facilitated the absorption of coumarin carried by nanoparticles into both the brain and the circulation while UEA I functionization only enhanced that into the brain and presented better brain-targeting efficiency. Distribution profiles of UEA-NP in the nasal cavity confirmed this deduction by showing clearly UEA-NP accumulated on the olfactory mucosa.

5. Conclusion

Lectin surface modification opened a novel pathway to improve the brain uptake of agents loaded by biodegradable PEG-PLA nanoparticles after nasal administration. UEA I, specifically binding to L-fucose, which is largely located in the olfactory epithelium in the nasal cavity, might serve as a promising targeting ligand for the brain drug delivery system following intranasal administration.

Acknowledgments

The study was supported by National Natural Science Foundation of China (30171112), National Doctoral Foundation of China (20050246073) and Innovation Foundation of Fudan University.

References

Bies, C., Lehr, C.M., Woodley, J.F., 2004. Lectin-mediated drug targeting: history and applications. Adv. Drug. Deliv. Rev. 56, 425–435.

Chen, H., Torchilin, V., Langer, R., 1996. Lectin-bearing polymerized liposomes as potential oral vaccine carriers. Pharm. Res. 13, 1378–1383.

Chen, X.Q., Fawcett, J.R., Rahman, Y.E., Ala, T.A., Frey II, W.H., 1998. Delivery of nerve growth factor to the brain via the olfactory pathway. J. Alzheimers Dis. 1, 35–44.

Desai, M.P., Labhasetwar, V., Walter, E., Levy, R.J., Amidon, G.L., 1997. The mechanism of uptake of biodegradable microparticles in Caco-2 cells is size dependent. Pharm. Res. 14, 1568–1573.

Dufes, C., Olivier, J.C., Gaillard, F., Gaillard, A., Couet, W., Muller, J.M., 2003. Brain delivery of vasoactive intestinal peptide (VIP) following nasal administration to rats. Int. J. Pharm. 255, 87–97.

Ellman, G.L., 1959. Tissue sulfhydryl groups. Arch. Biochem. Biophys. 82, 70–77.

Gao, X., Tao, W., Lu, W., Zhang, Q., Zhang, Y., Jiang, X., Fu, S., 2006. Lectin-conjugated PEG-PLA nanoparticles: preparation and brain delivery after intranasal administration. Biomaterials 27, 3482–3490.

Gheri, G., Gheri Bryk, S., Balboni, G.C., 1991. Sugar residues of glycoconjugates in the olfactory epithelium of the human fetus: histochemical study using peroxidase-conjugated lectins. Boll. Soc. Ital. Biol. Sper. 67, 781–788.

Graff, C.L., Pollack, G.M., 2005. Nasal drug administration: potential for targeted central nervous system delivery. J. Pharm. Sci. 94, 1187–1195.

Gref, R., Couvreur, P., Barratt, G., Mysiakine, E., 2003. Surface-engineered nanoparticles for multiple ligand coupling. Biomaterials 24, 4529–4537.

Illum, L., 2000. Transport of drugs from the nasal cavity to the central nervous system. Eur. J. Pharm. Sci. 11, 1–18.

Inamitsu, M., Nakashima, T., Uemura, T., 1990. Immunopathology of olfactory mucosa following injury to the olfactory bulb. J. Laryngol. Otol. 104, 959–964.

Jansson, B., Hagerstrom, H., Fransen, N., Edsman, K., Bjork, E., 2005. The influence of gellan gum on the transfer of fluorescein dextran across rat nasal epithelium in vivo. Eur. J. Pharm. Biopharm. 59, 557–564.

Kim, T.M., Chung, H., Kwon, I.C., Sung, H.C., Jeong, S.Y., 2000. In vivo gene transfer to the mouse nasal cavity mucosa using a stable cationic lipid emulsion. Mol. Cells 10, 142–147.

Lu, W., Zhang, Y., Tan, Y.Z., Hu, K.L., Jiang, X.G., Fu, S.K., 2005. Cationic albumin-conjugated pegylated nanoparticles as novel drug carrier for brain delivery. J. Control. Release 107, 428–448.

Lundh, B., Brockstedt, U., Kristensson, K., 1989. Lectin-binding pattern of neuroepithelial and respiratory epithelial cells in the mouse nasal cavity. Histochem. J. 21, 33–43.

Melgarejo Moreno, P., Hellin Meseguer, D., Melgarejo Moreno, C., 1998. Olfactory epithelium of the rat: lectin-mediated histochemical studies. An. Otorrinolaringol. IberoAm. 25, 471–480.

Ohtake, K., Maeno, T., Ueda, H., Natsume, H., Morimoto, Y., 2003. Poly-L-arginine predominantly increases the paracellular permeability of hydrophilic macromolecules across rabbit nasal epithelium in vitro. Pharm. Res. 20, 153–160.

Olivier, J.C., Huertas, R., Lee, H.J., Calon, F., Pardridge, W.M., 2002. Synthesis of pegylated immunonanoparticles. Pharm. Res. 19, 1137–1143.

Olivier, V., Meisen, I., Meckelein, B., Hirst, T.R., Peter-Katalinic, J., Schmidt, M.A., Frey, A., 2003. Influence of targeting ligand flexibility on receptor binding of particulate drug delivery systems. Bioconjugate Chem. 14, 1203–1208.

Panyam, J., Labhasetwar, V., 2003. Dynamics of endocytosis and exocytosis of poly(D,L-lactide-*co*-glycolide) nanoparticles in vascular smooth muscle cells. Pharm. Res. 20, 212–220.

Pardridge, W.M., 1991. Peptide Drug Delivery to the Brain. Raven Press, New York, pp. 99–122.

Pellier, V., Astic, L., 1994. Histochemical and immunocytochemical study of the migration of neurons from the rat olfactory placode. Cell Tissue Res. 275, 587–598.

Russell-Jones, G.J., Veitch, H., Arthur, L., 1999. Lectin-mediated transport of nanoparticles across Caco-2 and OK cells. Int. J. Pharm. 190, 165–174.

Sobal, G., Resch, U., Sinzinger, H., 2004. Modification of low-density lipoprotein by different radioiodination methods. Nucl. Med. Biol. 31, 381–388.

Takami, S., Getchell, M.L., Getchell, T.V., 1994. Lectin histochemical localization of galactose, *N*-acetylgalactosamine, and *N*-acetylglucosamine in glycoconjugates of the rat vomeronasal organ, with comparison to the olfactory and septal mucosa. Cell Tissue Res. 277, 211–230.

Teichberg, V.I., Aberdam, D., Erez, U., Pinelli, E., 1988. Affinity-repulsion chromatography. Principle and application to lectins. J. Biol. Chem. 263, 14086–14092.

Tobio, M., Gref, R., Sanchez, A., Langer, R., Alonso, M.J., 1998. Stealth PLA–PEG nanoparticles as protein carriers for nasal administration. Pharm. Res. 15, 270–275.

Vila, A., Sanchez, A., Tobio, M., Calvo, P., Alonso, M.J., 2002. Design of biodegradable particles for protein delivery. J. Control. Release 78, 15–24.

Vila, A., Sanchez, A., Evora, C., Soriano, I., McCallion, O., Alonso, M.J., 2005. PLA–PEG particles as nasal protein carriers: the influence of particle size. Int. J. Pharm. 292, 43–52.

Vyas, T.K., Shahiwala, A., Marathe, S., Misra, A., 2005. Intranasal drug delivery for brain targeting. Curr. Drug Deliv. 2, 165–175.

Yuan, J., 1993. Estimation of variance for AUC in animal studies. J. Pharm. Sci. 82, 761–763.

Zhang, Q., Jiang, X., Jiang, W., Lu, W., Su, L., Shi, Z., 2004. Preparation of nimodipine-loaded microemulsion for intranasal delivery and evaluation on the targeting efficiency to the brain. Int. J. Pharm. 275, 85–96.

Zhang, Y., Zhang, Q., Zha, L., Yang, W., Wang, C., Jiang, X., Fu, S., 2004. Preparation, characterization and application of pyrene-loaded methoxy poly(ethylene glycol)-poly(lactic acid) copolymer nanoparticles. Colloid Polym. Sci 282, 1323–1328.